Coupling 3D printing and novel replica molding for in house fabrication of skeletal muscle tissue engineering devices

Iuliano, A.; Wal, E. van der; Ruijmbeek, C.W.B.; in't Groen, S.L.M.; Pijnappel, W.W.M.P.; Greef, J.C. de; Saggiomo, V.

ADVANCED MATERIALS TECHNOLOGIES
www.advmattechnol.de

Coupling 3D Printing and Novel Replica Molding for In House Fabrication of Skeletal Muscle Tissue Engineering Devices

Alessandro Iuliano, Erik van der Wal, Claudine W. B. Ruijmbeek, Stijn L. M. in 't Groen, W. W. M. Pim Pijnappel, Jessica C. de Greef,* and Vittorio Saggiomo**

The transition from 2D to 3D engineered tissue cultures is changing the way biologists can perform in vitro functional studies. However, there has been a paucity in the establishment of methods required for the generation of microdevices and cost-effective scaling up. To date, approaches including multistep photolithography, milling and 3D printing have been used that involve specialized and expensive equipment or time-consuming steps with variable success. Here, a fabrication pipeline is presented based on affordable off-the-shelf 3D printers and novel replica molding strategies for rapid and easy in-house production of hundreds of 3D culture devices per day, with customizable size and geometry. This pipeline is applied to generate tissue engineered skeletal muscles in vitro using human induced pluripotent stem cell-derived myogenic progenitors. These production methods can be employed in any standard biomedical laboratory.

1. Introduction

The increasing popularity gained by 3D cell culture systems in life sciences finds its explanation in the possibility of mimicking the native structure and function of a tissue in vitro.[1] Unsurprisingly, more and more research groups started investing resources and expertise in the generation of 3D in vitro models for various tissues.[2–10] Adopting this paradigm is particularly significant for contractile and load-bearing tissues, such as tendons, cardiac, and skeletal muscle.[11–14] However, since the criteria for a transition from monolayer cultures to 3D systems were first outlined more than ten years ago,[15,16] cost-effective ways for easy production of 3D cell culture systems are still lacking. Ideally, for a broader use, 3D cell culture systems should be simple, versatile and applicable in standard biomedical laboratories independently of specific biofabrication expertise.

For adequate lodging of 3D contractile tissues, flexible pillars are preferred to promote maturation and to provide tendon-like attachment points for contraction.[17] Compared to alternative methods, such as micropatterned surfaces,[18,19] flexible pillars offer mechanical and functional advantages in the tracking of their displacement as a consequence of a tissue's contraction.[17] Downscaling the size of engineered tissues is also possible by producing pillars in a T-shape: "caps" on top of each pillar help the retention of smaller tissues under tension.[5–7,17] Multistep photolithography has been used to generate negative molds for polydimethylsiloxane (PDMS) T-shaped pillars.[5–7] However, this approach carries a limitation in the production of features larger than few hundreds of micrometers and lacks versatility: producing a single master mold is time-consuming and expensive, requiring most of the

A. Iuliano, C. W. B. Ruijmbeek, S. L. M. in 't Groen, Dr. W. W. M. P. Pijnappel
Department of Clinical Genetics
Erasmus University Medical Center
Rotterdam 3015 GE, Netherlands
E-mail: w.pijnappel@erasmusmc.nl

A. Iuliano, C. W. B. Ruijmbeek, S. L. M. in 't Groen, Dr. W. W. M. P. Pijnappel
Department of Pediatrics
Erasmus University Medical Center
Rotterdam 3015 GE, Netherlands

The ORCID identification number(s) for the author(s) of this article can be found under https://doi.org/10.1002/admt.202000344.

DOI: 10.1002/admt.202000344

A. Iuliano, C. W. B. Ruijmbeek, S. L. M. in 't Groen, Dr. W. W. M. P. Pijnappel
Center for Lysosomal and Metabolic Diseases
Erasmus Medical Center
Rotterdam 3015 GE, Netherlands

Dr. E. van der Wal, Dr. J. C. de Greef
Department of Human Genetics
Leiden University Medical Center
Leiden 2333 ZA, Netherlands
E-mail: J.C.de_Greef@lumc.nl

Dr. V. Saggiomo
Department of BioNanoTechnology
Wageningen University and Research
Wageningen 6708 WG, Netherlands
E-mail: vittorio.saggiomo@wur.nl

time dedicated facilities such as clean rooms. To avoid multistep photolithography, molds have been generated using single-step lithography[8–10] or milled Teflon.[19] This was followed by manually gluing a thin square of PDMS on top of each pillar for obtaining the T-shape, making this method time-consuming and not prone to high throughput. A multiple step aluminum mold has recently been used to fabricate hammer-like PDMS pillars.[20] In this case, high throughput was obtained at the expense of versatility, as each variation in size and shape of the pillars would require a new micromilled aluminum mold. Hydrogel 3D printing[21] involves 3D printers that are expensive, difficult to operate, and not accessible for standard biomedical laboratories. Recently, a set of devices containing small hook-shaped pillars has been created using a 3D printer, however, this method involved an expensive machine and was only partially successful due to the replica molding strategy based on hard, plastic molds.[22] Finally, it is possible to fabricate pillars-equipped devices directly in plastic materials using affordable, off-the-shelf 3D printers, but these products are too rigid to allow contractile measurements in a noninvasive way.[23,24]

Here, we present fast and versatile methods which combine 3D printing and innovative replica molding for the in house realization of three PDMS culture chambers of different sizes, complexity, and throughput. We applied these to the generation of 3D tissue engineered skeletal muscles (TESMs) derived from human induced pluripotent stem cells (hiPSCs).[25,26] The first device was the largest, contained straight pillars and fitted in a 12-well plate. It was generated by simply peeling off the replica from a negative mold 3D printed using a 2k €, off-the-shelf fused deposition modeling (FDM) machine. In this method, the intrinsic properties of 3D printing allowed a high degree of versatility compared to other techniques, such as injection molding, for the fabrication of the negative mold. In injection molding,[27,28] each variation on the design must be followed by the fabrication of a new metal mold, making the process expensive and not comparably versatile. The second device was intermediate sized, contained T-shaped pillars, and was suitable for 24-well plates. It was generated using the same printer but included the dissolution of the mold to preserve the T-shape.[29] The third, smallest device fitted 48-well plates and involved a stereolithography 3D printer (SLA) of ≈3k € or even one of ≈500 €. A novel replica molding strategy was used to preserve the finest details via a highly stretchable mold composed of the polymer Ecoflex. These last two methodologies are used to fabricate T-shaped pillars in one single demolding step, which, due to the geometry of the pillars would be impossible to achieve in a hard mold made using, for example, injection molding. Hundreds of final PDMS 3D culture chambers from the same mold could be obtained without losing details and without the need for additional fabrication steps.

2. Results

2.1. FDM 3D Printer: Direct Peeling Method

The first design consisted of a 3D culture chamber of 50 µL in a "dog-bone" shape of a total length of 11 mm, provided with two cylindrical pillars of 1 mm in diameter and 3.2 mm in height (**Figure 1**a-i; Figure S1a, Supporting Information). This model was designed to be devoid of any overhanging feature of micrometric size, in order to be directly peeled from the 3D printed negative master mold during the replica molding without incurring any damage to the final PDMS structure. A circular-based negative structure provided with a set of 23 chambers (Figure 1a-ii) was 3D printed using an Ultimaker 2+ equipped with a 250 µm nozzle (Figure S2, Supporting Information). The circular shape of the base was chosen to fix the printed mold inside a 60 mm plastic Petri dish for convenient PDMS casting during the replica molding step (Figure S3, Supporting Information). For this method, either polylactic acid (PLA) or acrylonitrile butadiene styrene (ABS) can be used as thermoplastic materials in 3D printing. However, PLA has a lower melting point compared to ABS and it can deform during the curing of the PDMS (>50 °C). This method proved to be remarkably fast and user friendly, however, it carries one main limitation: the impossibility to obtain replicas with more complex geometries due to the mechanical damage that the peeling from a rigid mold can cause.[22] The hard, nondeformable mold makes the retention of features such as long and thin or T-shaped pillars arduous. This obstacle led us to develop the next two methods.

2.2. FDM 3D Printer: ESCARGOT Method

Increasing the number of samples for experimental necessities often means reducing the volume of the sample itself (e.g., from a 12-well plate to a 48-well plate). However, reducing the diameter of a pillar can cause a contractile tissue to slip away from it due to the tension to which the bundle is subjected during culture.[17,22] Hence the necessity to incorporate a protrusion in the pillar's design arises, leading to the more complex T-shaped pillar suitable for supporting small tissues. To this end, a negative model consisting of a smaller, 8 mm long chamber of 30 µL with pillars of 750 µm in diameter and 3.2 mm in height in a T-shape was realized (Figure 1b-i; Figure S1b, Supporting Information). To obtain a PDMS replica of such structure while still using FDM printing, we adapted another approach previously used in the fabrication of microfluidic systems in a monolithic PDMS.[29] This method, called Embedded Scaffold RemovinG Open Technology (ESCARGOT), replaces the peeling with the dissolution of a sacrificial mold by exploiting the solubility of ABS in acetone. Briefly, an ABS FDM-printed negative master mold (Figure 1b-ii) was immersed in liquid PDMS, leaving at least one portion of the structure exposed. Once the PDMS was cured, the ABS scaffold was dissolved in an acetone bath overnight (Figure S4, Supporting Information). The resulting PDMS positive structure retains all the features of the original model (Figure 1b-iii,iv), which would have been lost if directly peeled from the 3D printed master.

This method was developed to solve the problems related to the need of smaller and more complex shapes of pillars, while still making use of the same 3D printing setup. However, for reproducible fabrication of pillars with a diameter smaller than 750 µm a different printing system must be used.

2.3. SLA 3D Printer: Ecoflex Replica Method

The generation of 3D culture chambers with 15 µL volumetric capacity, containing T-shaped pillars with a diameter of 500 µm and a height of 2.5 mm (Figure S1c, Supporting Information) was made possible employing a new method, which combines

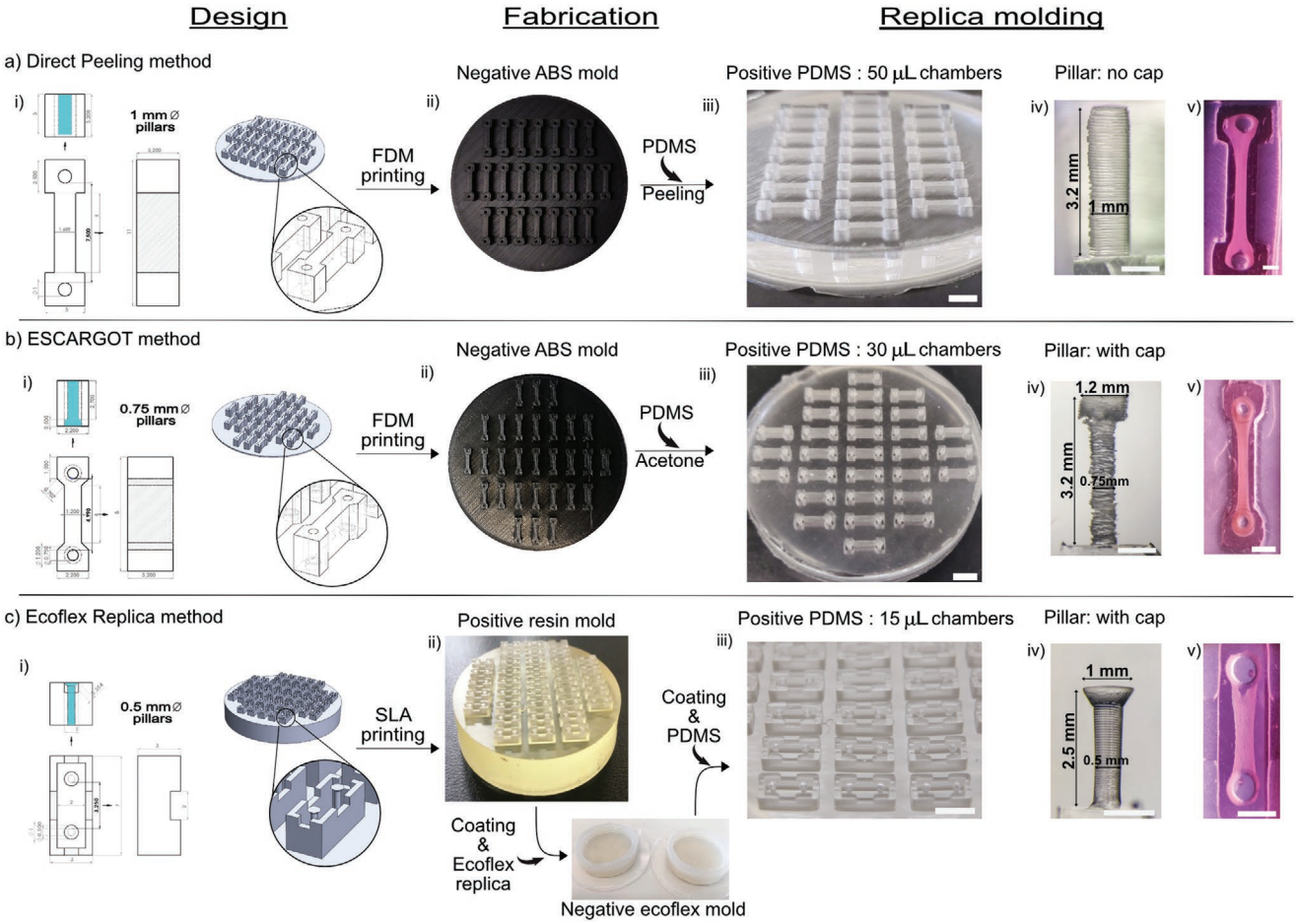

Figure 1. Fabrication methods of the 3D culture chambers for tissue engineered skeletal muscles. a) Direct Peeling method. Technical drawing of a single chamber and 3D CAD model of the negative master mold (i), 3D printed ABS negative master mold through fused deposition modeling (FDM) printing (ii), detail of a PDMS positive replica (iii), detail of the pillar (iv). b) ESCARGOT method. The same process of the Direct Peeling method from design to 3D printed mold is shared (i-ii), detail of PDMS replica (iii) and of a T-shaped pillar with cap, obtained after the dissolution of the ABS master mold (iv). c) Ecoflex Replica method. Technical drawing of a single chamber and 3D CAD model of the positive master mold (i), 3D printed resin positive master mold through stereolithography (SLA) printing (top), negative molds in form of replicas made of Ecoflex (bottom), detail of a PDMS positive replica (iii) and a T-shaped pillar provided with conical cap (iv). a–c) Examples of tissue engineered skeletal muscles within the three different PDMS chambers (v). Scale bars: a–c) 5 mm (iii), 1 mm (iv, v).

SLA printing and fully deformable elastic molds (Figure 1c). SLA printers use a laser source to photo-crosslink a liquid polymeric resin, usually composed of acrylates, layer by layer. Thanks to the smaller laser spot, they are not only able to generate smaller features and thinner layers than FDM (down to 200 and 25 µm, respectively), but also to create complex geometries with overhanging structures. SLA printers are usually more expensive than FDMs, however, recently a new category of printers called masked SLA (mSLA) has been introduced to the consumer market. In these machines an array of 405 nm UV-LED replaces the laser source, contributing to diminish their price to below 500€.

Despite the improved resolution of SLA printers, it remains considerably difficult to directly peel the PDMS replicas from the 3D-printed rigid molds without damaging the micrometric features. We addressed this issue by generating an intermediate "carrier" mold made of the highly elastic polymer Ecoflex 00–30. Ecoflex is a cheap, stretchable, and durable silicone, mostly used in soft robotics, which can be stretched over 900% before breakage.[30,31] Thanks to its properties, we used Ecoflex as negative mold to produce PDMS replicas. By means of a Formlab Form 2 SLA or a Photon Anycubic mSLA, we 3D printed a positive master comprehending 37 culture chambers of 7 × 2.5 × 3 mm ($L \times H \times W$) equipped with 2.5 mm long T-shaped pillars of 500 µm diameter, provided with conical caps (Figure 1c-i,ii; **Figure 2**a; Figures S5–S7, Supporting Information). This particular size of pillar was chosen as optimization experiments showed that a larger diameter (resulting in a higher stiffness) could cause breakage of the tissues as a result of spontaneous contractions (data not shown). In contrast with the dog-bone shape of the previous two designs, developed to provide a spindlier shape to the tissues, a rectangular shape was chosen for the third model. This was the result of prior optimization experiments which saw the maintaining of a dog-bone shape in the smallest, 15 µL format to be counterproductive for a homogeneous spread of the hydrogel within the chamber, due to surface tension caused by the closer PDMS walls.

After the 3D printing step, the negative mold was then generated through Ecoflex Replica molding (Figure 1c-ii,iii;

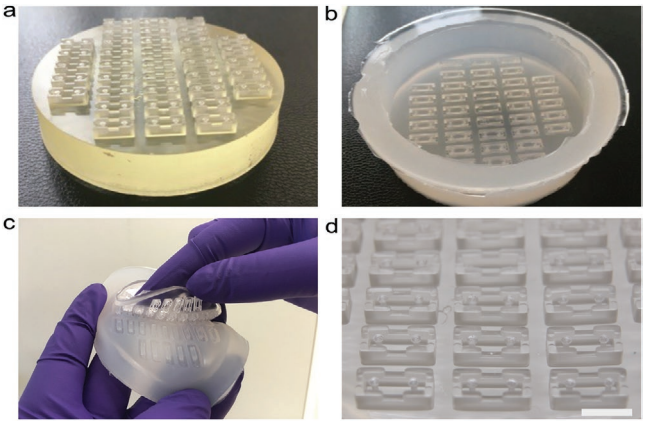

Figure 2. Generation of 3D culture chambers through the Ecoflex Replica method. a) Positive master mold in acrylate resin produced with SLA 3D printing. b) Single negative replica obtained by pouring liquid Ecoflex on the 3D printed positive master, after curing of the elastomer. c) Ecoflex replica molding: PDMS was poured inside the Ecoflex negative mold. After curing the PDMS, the mold was stretched, allowing easy peeling of the PDMS positive replica. d) Detail of the PDMS positive replica: the micrometric features of the chambers and the caps on the pillars are retained. Scale bar: d) 5 mm.

Figure 2b) and the final positive PDMS was easily peeled off after stretching the Ecoflex mold (Figure 1-iii; Figure 2c,d). Both the 3D printed positive and the Ecoflex negative molds were subjected to a perfluorodecyltrichlorosilane (PFOTS) coating, which facilitates the unmolding process by making their respective surfaces inert (Figure S5, Supporting Information).[32]

The final PDMS replicas are a perfect copy of the original 3D printed structures without any detectable variation. There could be small variability between different printed positives, as a result of intrinsic characteristics of 3D printing. Multiple replicas from the same mold appear identical (**Figure 3**) and even after 14 cycles, it is still possible to distinguish the single pixels (47 µm) of the Anycubic Photon 3D printer (Figures S8–S10, Supporting Information). We found that the dimensional differences between the replicas are in the order of less than 10 µm, within the error of a bright field microscope on a nonflat object as shown by the overlay of different replicas in Figure 3, therefore we estimated that the difference between the replicas is below 5%. However, being subjected to reiterated mechanical and thermal stresses, Ecoflex intermediate molds appear to acquire structural wear over time, leading to a possible difficult peeling off or microcracks in the Ecoflex (Figure 3; Figure S9, Supporting Information). Due to the multiple variables involved in the method, such as temperature and time spent in the oven, cooling time and ramping between different temperatures, stretching in different directions and so on, it is difficult to predict when microcracks will affect the Ecoflex mold. Nevertheless, we found that a single Ecoflex mold with 37 chambers could be reused at least 15 times without issues, yielding over 500 3D chambers with intact T-shaped pillars.

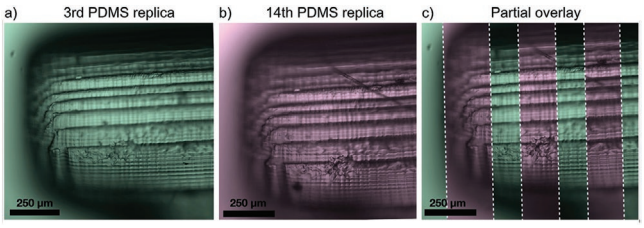

Figure 3. Structural integrity of Ecoflex replica products after several cycles of replica molding, bright field micrographs. a) Third replica obtained from the same Ecoflex mold, b) 14th replica from the same Ecoflex mold and c) a partial overlay of the two micrographs. Scale bars: a–c) 250 µm.

2.4. Generation of Tissue Engineered Skeletal Muscles (TESMs)

We next determined if the generated 3D tissue chambers were able to promote the formation of TESMs and if downscaling affects formation of 3D tissues. TESMs were generated by mixing a suspension of hiPSC-derived myogenic progenitors with a biocompatible hydrogel constituted of fibrin and Matrigel (see Experimental Section) developed by adapting a previously published protocol.[4] Corresponding volumes of 50, 30, and 15 µL of cell-laden hydrogel were directly pipetted in the chambers obtained from the Direct Peeling method, ESCARGOT method, and Ecoflex Replica method, which were fixed inside the wells of a 12-well plate, 24-well plate, and 48-well plate, respectively (**Figure 4**). As an example, from an initial cell-hydrogel volume of 500 µL, it was possible to cast 10 units of 50 µL TESMs, 16 units of 30 µL TESMs, while from the same volume 33 TESMs could be casted in the devices obtained with the Ecoflex Replica method. In the first 2 d after casting, the cell-laden hydrogel underwent visible compaction (Figure S11, Supporting Information). After 7 d of differentiation, TESMs were fixed, immunostained and analyzed by confocal imaging (see Experimental Section). Engineered tissues in all the 3D culture systems showed a comparable organization, characterized by the presence of long, aligned and multinucleated myofibers that stained positive for the sarcomeric protein titin (Figure 4b,e,h), whose typical striated pattern was immediately recognizable (Figure 4c,f,i). Myofibers of the TESMs cultivated in the three different devices showed comparable thickness at 7 d of differentiation, as shown in Figure 4j, indicating that the chamber structure had no major impact on the growth of TESMs.

3. Discussion

We presented a fabrication pipeline based on off-the-shelf 3D printers, comprehending three methods to generate PDMS-based tissue engineering culture devices. We aimed to highlight the profound adaptability of our approach by producing 3D culture chambers with different sizes and levels of complexity to support the maturation of TESMs (**Figure 5**). The three methodologies presented here are different from directly 3D printed microfluidic devices[23] as the latter produce hard plastic pillars which are not suitable for noninvasive force measurements. The advantages of our methodologies are not only production scale, but also manufacturing versatility and simplicity. In addition, the techniques employed here preserved microstructures without special processes, due to the peeling of a soft elastomer

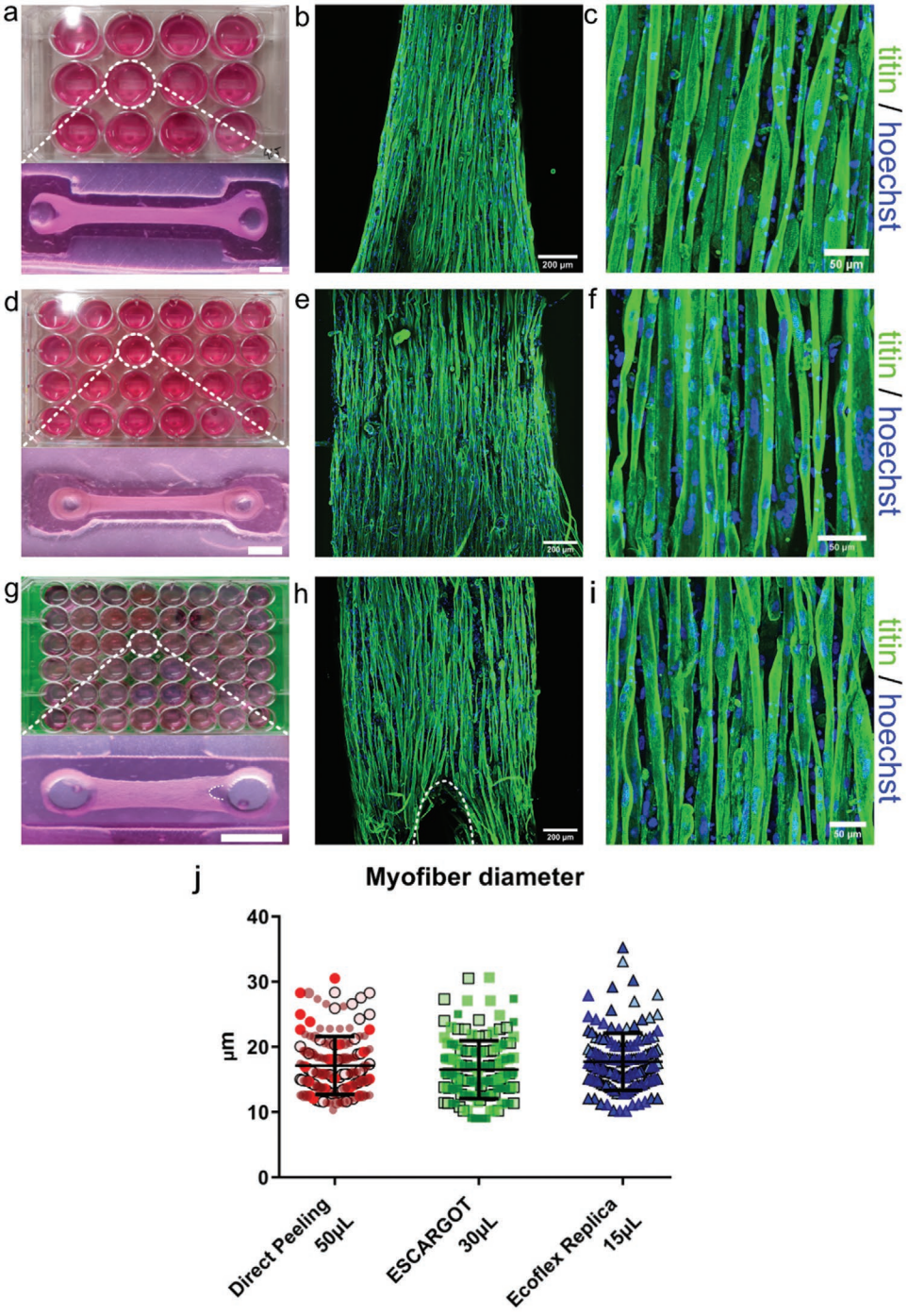

Figure 4. Tissue engineered skeletal muscles (TESMs) of different sizes generated with the three different 3D culture chambers. a–c) 12-well plate containing TESMs within the 50 µL chambers obtained with the Direct Peeling method. b) Tissues were stained for the sarcomeric protein titin after 7 d of differentiation. c) The typical sarcomeric striation pattern of titin is visible at higher magnifications. d) Smaller, 30 µL TESMs, obtained from the ESCARGOT fabricated chambers, inside a 24-well plate. e) Engineered tissues display a similar morphology as in b with millimeters-long myofibers with f) evident sarcomeric striation. g) A 48-well plate including TESMs generated in the 15 µL chambers fabricated with the Ecoflex Replica method. h,i) Even in the smallest tissue, myogenic progenitors differentiated in long, multinucleated myofibers with an organized titin pattern. g,h) The dashed curved line at one extremity of the TESM indicates a loop-like structure originated from the tension to which the tissue is subjected. j) TESMs of different size differentiated for 7 d showed that myofibers in all three devices have a similar diameter with an average of ≈17 µm. Each element in the plot represents a single measurement, each color represents a single biological replica ($n = 3$). SD ± = 4457 for Direct Peeling; ± = 4450 for ESCARGOT; ± = 4374 for Ecoflex replica. Scale bars: a,d,g) 1 mm; b,e, h) 200 µm; c, f,i) 50 µm.

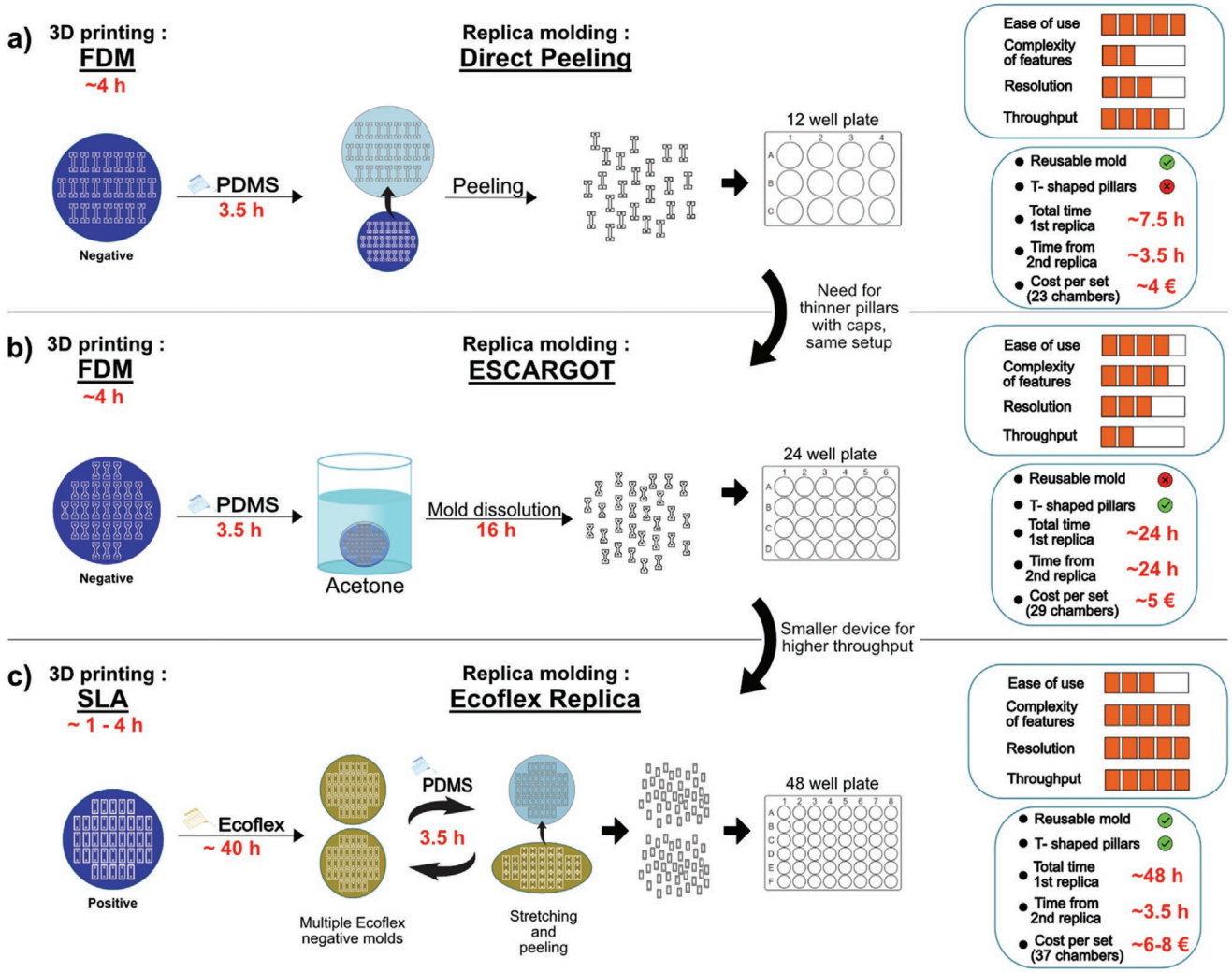

Figure 5. Overview of the different fabrication methods. a) The Direct Peeling method is the fastest and easiest to the operator, involving a simple design and a reusable negative master mold, thus maintaining a noticeable low cost. This method has a high throughput as the 3D printed mold can be reused multiple times. b) With the same FDM setup, in the second method it is possible to generate thinner pillars provided with caps still in a single demolding step. In this case, the 3D printed sacrificial mold is dissolved in acetone, therefore not reusable, with a slight increase in production cost and decrease in throughput. c) For higher throughput applications, the Ecoflex Replica method allows both an increment of resolution and production, thanks to the use of the SLA printer and the stretchable and reusable negative molds. The 3D printed positive mold can be used multiple times too, to fabricate multiple negative Ecoflex molds, further increasing the throughput of the method. (a-c). All the three methods can be operated in any standard biomedical laboratory without the need of specific biofabrication expertise. Ease of use indicates the number of steps and equipment required to obtain a certain device; complexity of features refers to the multiplicity of features that can be simultaneously incorporated in the final product; resolution indicates the capacity of the 3D printer to print small details; throughput indicates the number of devices that can be produced per unit of time and their suitability for standard multiwell systems. The costs of the fabrication materials are comparably low for each method.

or the dissolution of the hard mold. These fabrication methods can be performed in any biological laboratory without any expensive facilities.

The structures realized with the Direct Peeling method can be produced with other fabrication techniques, such as milling[19] or injection molding,[27,28] thanks to their millimetric dimensions. However, 3D printing offers higher versatility, as the fabrication process can be fully tuned in house from design to manufacturing to fit different needs and possible new necessities naturally arising during research. A perfect example of this versatility is represented by the second method, developed using the same FDM printing setup but implementing the ESCARGOT strategy. To meet the need of thinner, T-shaped pillars provided with "caps" for a better retention of smaller engineered muscles, the ABS plastic molds were dissolved in acetone leaving the features intact. With "Direct Peeling" and "ESCARGOT," 7.5 and 24 h, respectively, are required to obtain enough PDMS devices for multiple experiments. The time employed for the first replica in the Direct Peeling method decreases after the second one, as the 3D printed master remains. The ESCARGOT method, conversely, requires more time as the master needs to be 3D printed after each use (Figure 5a,b; Tables S1 and S2, Supporting Information).

In the Ecoflex Replica method, SLA 3D printing was employed to further downscale the system with increased reproducibility for higher throughput applications. The devices produced with SLA 3D printing include the simultaneous presence of millimetric and micrometric features, a combination hardly possible with techniques such as photolithography, which is confined to the realization of structures within hundreds of micrometers.[5–10] To replicate such structures in PDMS, here for the first time the highly elastic polymer Ecoflex[30,31] is applied as a reusable replica molding substrate for tissue engineering applications. To avoid accidental damage during demolding, conventional procedures typically require supplementary steps solely to fix caps on each pillar[9,10,33] or serial replica molding stages with high risk of failure.[22] Here, in around 48 h from design to final product, we inexpensively produced hundreds of faithful replicas with T-shaped pillars without additional fabrication steps thanks to the implementation of the stretchable molds. Also in this case, like the Direct Peeling method, the time invested after the first replica decreases considerably, as both the 3D printed mold and the Ecoflex molds can be reused multiple times (Figure 5c, Table S3, Supporting Information). Considering the aforementioned advantages, the low cost and the simplicity of use, the Ecoflex Replica strategy can potentially be employed in a wider spectrum of applications: from the creation of supporting devices for other contractile or load bearing tissues such as heart and tendons, to the direct use as soft substrate for specific cell culture needs.

The versatility, speed, low cost, and ease of use of our methods could promote a larger diffusion of tissue engineering approaches in biomedical laboratories, and their implementation as tools for basic research, disease modeling, and drug screening.

4. Experimental Section

Fabrication of the PDMS-Based 3D Culture Platforms: 3D models of each design were generated using the CAD software SolidWorks (2017, Dassault Systèmes, France). For the FDM printed devices, 3D models were converted in .gcode format using the software Ultimaker Cura (Ultimaker, Netherlands) and then uploaded to the 3D printer. For the SLA printed master molds, 3D models were sliced using the software PreForm (Formlabs, USA) and Anycubic slicer (Anycubic, China) (see Supporting Information).

Direct Peeling Method: 3D printing was performed using an Ultimaker 2+ (Ultimaker, Netherlands) FDM 3D printer, equipped with acrylonitrile butadiene styrene (ABS, Ultimaker) plastic, a nozzle with 0.250 mm diameter, a layer thickness of 0.060 mm and a controlled extruding temperature of 240 °C.

Polydimethylsiloxane (PDMS, Dow Corning, MI) was prepared by mixing the prepolymer with the curing agent in a 10:1 w/w ratio (as recommended by the manufacturer). Uncured elastomer was first degassed for 10 min and then poured directly on the ABS molds. Subsequently it was subjected to a second 20 min degassing step in order to remove any possible trapped air bubble and finally cured at 75 °C in a ventilated oven for at least 3 h. Cured PDMS replicas were carefully peeled from the ABS molds and quickly washed in isopropanol to remove any impurities.

ESCARGOT Method: Fabrication of the ABS molds was performed adopting the same procedure and parameters used for the Direct Peeling method. After pouring the premixed and degassed PDMS on the negative molds, the elastomer was cured at 75 °C in a ventilated oven for at least 3 h. ABS dissolution was achieved by immersing the 3D printed negative master overnight in an acetone bath, together with its PDMS replica still attached. The following day, complete removal of ABS was helped by washing the PDMS replica under running acetone flow for few seconds followed by a quick rinse with isopropanol.

Ecoflex Replica Method: SLA printing was performed both by means of a Form2 (Formlabs, USA) using grey resin v4 (Formlabs, USA) and a layer thickness of 0.050 mm and of an Anycubic Photon using Anycubic 405 UV clear resin (Anycubic, China) and a layer thickness of 0.050 mm. After printing, the SLA products were first left in isopropanol for 20 min and in ethanol (EtOH) for 10 min and finally rinsed with EtOH. The prints were dried with compressed air and postcured in an 80 W UV chamber for 10 min. The 3D printed master molds were then coated with trichloro(1H, 1H, 2H, 2H-perfluorooctyl)silane (PFOTS, 97%, Merk) using chemical vapor deposition (CVD) in a vacuum desiccator: the 3D printed structure was first air plasma activated for 30 s, then placed in a desiccator with a vial of 100 µL of PFOTS and high vacuum was applied. The desiccator was then left under static vacuum overnight for CVD. After PFOTS deposition, the 3D printed structure was removed from the desiccator and left in the oven at 70 °C for 1 h and finally washed with EtOH and isopropanol.

Ecoflex 00–30 (Smooth-On Inc., PA) intermediate mold was generated by pouring the two premixed liquid pre-polymers (1A:1B) on the 3D printed structure, followed by a degassing step inside a vacuum desiccator for 15 min. After degassing, platforms were left curing at room temperature (RT) for 8 h and then they were peeled off the 3D printed master mold. The Ecoflex mold was washed with EtOH and rinsed dry with compressed air. Before being utilized as negative molds for PDMS replica molding, Ecoflex molds were subjected to a PFOTS CVD coating using the same procedure used for the CVD of the 3D printed master mold.

Finally, PDMS replicas were obtained by pouring uncured PDMS on the Ecoflex molds and curing it at 75 °C in a ventilated oven for at least 3 h. The PDMS replicas removing procedure involved simple manual stretching of the elastic molds, which spontaneously induces the peeling of the PDMS structures.

In order to be utilized for 3D cell culture, each PDMS chamber of each method was cut from the whole PDMS block and fixed inside wells of 12, 24, or 48 well plates (CELLSTAR, Greiner Bio-One, Germany) using PDMS (10:1) as glue and allowing it to solidify for 1 h at 70 °C. All the PDMS replicas from each fabrication method were sterilized by rinsing in 70% ethanol for 15 min followed by 3× PBS washing and by UV treatment for 15 min, immediately before usage in cell culture.

2D Culture of hiPSC-Derived Myogenic Progenitors: hiPSC-derived myogenic progenitors were generated following a previously published protocol[25,26] and cultured accordingly. Briefly, cells were expanded in monolayer culture in myogenic progenitor proliferation medium, consisting of DMEM high glucose (Gibco, Waltham, MA) supplemented with 10% FBS (Hyclone, US), 1% penicillin–streptomycin–glutamine (P/S/G) (Gibco, Waltham, MA) and 100 ng mL^{-1} bFGF2 (Prepotech, Rocky Hill, NJ); medium was refreshed every 48 h. Culture dishes of 100 mm (CELLSTAR, Greiner Bio-One, Germany) were coated with ECM extract (1:200 diluted, Sigma-Aldrich, E6909) 40 min prior seeding. For passaging and harvesting, cells were detached in the incubator at 37 °C and 5% CO_2 with TrypLE reagent (Gibco, Waltham, MA) diluted 1:1 with PBS (Gibco, Waltham, MA).

Generation of 3D Human Tissue Engineered Skeletal Muscles: The hydrogel generated as extracellular matrix for the 3D culture was composed of bovine fibrinogen (Sigma-Aldrich) dissolved in DMEM high glucose (final concentration: 2 mg mL^{-1}), Matrigel growth factor reduced (20% v/v, Corning Life Sciences, Netherlands), thrombin from human plasma (Sigma-Aldrich) dissolved in 0.1% BSA in PBS (1% v/v, 0.5 U mL^{-1} final concentration), myogenic progenitor proliferation medium (69% v/v). Matrigel, previously stored at −20 °C, was kept at 4 °C 2 h before usage; fibrinogen, stored at −80 °C, was kept at 4 °C 1 h before usage. After detachment from culture dishes, cells were suspended in myogenic progenitor proliferation medium at a concentration of 16×10^6 cells mL^{-1} and the suspension was then mixed with fibrinogen and Matrigel. Last, thrombin was added to the

mix immediately before pipetting the cell-hydrogel mix into the PDMS chambers, which were coated with Pluronic F-127 (Sigma-Aldrich) for 1 h at RT to prevent unwanted adhesion of the hydrogel. A volume of 50, 30, and 15 µL was used for each TESM in the chambers obtained with the Direct Peeling, ESCARGOT, and Ecoflex Replica methods, respectively. All the hydrogel components, as well as tubes and micropipette tips, were kept on ice prior and during the duration of the experiments. The final solution was then left to polymerize for 30 min in the incubator at 37 °C and 5% CO_2, before adding the myogenic progenitors proliferation medium supplemented with 6-aminocaproic acid (1.5 mg mL^{-1}, Sigma-Aldrich). After 48 h, proliferation medium was switched to TESM differentiation medium, consisting of DMEM high glucose supplemented with 1% knock-out serum replacement, 1% ITS-X (all Gibco), 1% penicillin-G (Sigma-Aldrich), 1% Glutamax (Sigma-Aldrich), 6-aminocaproic acid (1.5 mg mL^{-1}, Sigma-Aldrich). Half volume of the TESM differentiation medium was replaced every 48 h. TESMs were kept on agitation at 55 rpm (Celltron orbital shaker, Infors HT, Switzerland) at 37 °C and 5% CO_2.

Immunofluorescent Stainings: Samples were fixed in 4% paraformaldehyde (PFA, Sigma-Aldrich) for 1 h at RT and then washed with PBS for three times. For whole-mount immunostaining, fixed samples were first subjected to a permeabilization/blocking step in a solution containing 0.5% Triton-X in PBS, 3% BSA in PBS, 0.1% Tween 20 in PBS on agitation, for 1 h at RT. After washing with PBS, samples were incubated with primary antibody for titin, 9D 10-s (IgM, 1:50, DSHB, IA), in 0.1% Triton-X in PBS, 0.1% BSA (Sigma-Aldrich) in PBS, 0.1% Tween 20 in PBS at RT for 1 h. Before incubation with the secondary antibody Alexa Fluor 488 (anti IgM, 1:500, Thermo Fisher Scientific, Waltham, MA), samples were washed in 0.1% Tween in PBS for 2 min and subsequently in PBS for 2 min. Secondary antibodies were diluted in the same solution used for the primary antibodies and samples were incubated for 1 h at RT. Last, nuclear staining was performed through incubation with Hoechst 33 342 (1:15 000, Sigma-Aldrich) at RT for 15 min followed by washing in PBS. Samples were kept in PBS at 4 °C before imaging.

Imaging Analysis of IF Stained Samples: Stained samples were imaged using a Leica TCS SP5 confocal microscope (Leica, Germany) equipped with LAS software (Leica, Germany), using 10× and 20× magnifications. Images were then analyzed using ImageJ version 1.52i. Myofiber size was measured using ImageJ and data analyzed using GraphPad Prism 6.

Data and Materials Availability

All data needed to evaluate the conclusions in the paper are present in the paper and/or the Supporting Information. Additional data related to this paper may be requested from the authors.

Supporting Information

Supporting Information is available from the Wiley Online Library or from the author.

Acknowledgements

The collaboration project is co-funded by the PPP Allowance made available by Health-Holland, Top Sector Life Sciences & Health, to the Prinses Beatrix Spierfonds to stimulate public-private partnerships (project numbers LSHM17075 and LSHM19015). The authors thank the Wageningen Electron Microscopy Centre for their support with the SEM measurements. The authors also thank Prof. Dr. Carlijn V.C. Bouten from Eindhoven University of Technology for the important initial input on the tissue engineering of skeletal muscle.

Author Contributions

A.I. and E.v.d.W. contributed equally to this work. W.W.M.P.P., J.C.d.G., and V.S. are shared senior authors. A.I., E.v.d.W., and V.S. carried out the design and fabrication of the devices. A.I., E.v.d.W., V.S., S.L.M.in 't.G., and C.R. performed the experiments. W.W.M.P.P., J.C.d.G., and V.S. conceptualized and supervised the work. All authors contributed to data analysis, discussion and interpretation. A.I., E.v.d.W., V.S., J.C.d.G. and W.W.M.P.P. wrote the manuscript with input from all the authors.

Conflict of Interest

The authors declare no conflict of interest.

Keywords

3D printing, hiPSCs, replica molding, skeletal muscles, tissue engineering

Received: April 13, 2020
Revised: June 8, 2020
Published online: July 26, 2020

[1] V. Marx, *Nature* **2015**, *522*, 373.
[2] H. Vandenburgh, M. Del Tatto, J. Shansky, J. Lemaire, A. Chang, F. Payumo, P. Lee, A. Goodyear, L. Raven, *Hum. Gene Ther.* **1996**, *7*, 2195.
[3] C. A. Powell, B. L. Smiley, J. Mills, H. H. Vandenburgh, *Am. J. Physiol.: Cell Physiol.* **2002**, *283*, C1557.
[4] S. Hinds, W. Bian, R. G. Dennis, N. Bursac, *Biomaterials* **2011**, *32*, 3575.
[5] W. R. Legant, A. Pathak, M. T. Yang, V. S. Deshpande, R. M. McMeeking, C. S. Chen, *Am. J. Ophthalmol.* **1983**, *95*, 552.
[6] A. Ramade, W. R. Legant, C. Picart, C. S. Chen, T. Boudou, *Methods Cell Biol.* **2014**, *121*, 191.
[7] B. Kalman, C. Picart, T. Boudou, *Biomed Microdevices* **2016**, *18*, 43.
[8] G. Agrawal, A. Aung, S. Varghese, *Lab Chip* **2017**, *17*, 3447.
[9] T. Osaki, S. G. M. Uzel, R. D. Kamm, *Sci. Adv.* **2018**, *4*, eaat5847.
[10] T. Osaki, S. G. M. Uzel, R. D. Kamm, *Nat. Protoc.* **2020**, *15*, 421.
[11] R. L. Lieber, J. Fridén, *Muscle Nerve* **2000**, *23*, 1647.
[12] H. H. Vandenburgh, P. Karlisch, L. Farr, *In Vitro Cell. Dev. Biol.* **1988**, *24*, 166.
[13] J. M. Jones, D. J. Player, N. R. W. Martin, A. J. Capel, M. P. Lewis, V. Mudera, *Front. Physiol.* **2018**, *9*, 483.
[14] N. M. Wragg, D. J. Player, N. R. W. Martin, Y. Liu, M. P. Lewis, *Biotechnol. Bioeng.* **2019**, *116*, 2364.
[15] F. Pampaloni, E. G. Reynaud, E. H. K. Stelzer, *Nat. Rev. Mol. Cell Biol.* **2007**, *8*, 839.
[16] N. F. Huang, V. Serpooshan, V. B. Morris, N. Sayed, G. Pardon, O. J. Abilez, K. H. Nakayama, B. L. Pruitt, S. M. Wu, Y. sup Yoon, J. Zhang, J. C. Wu, *Commun. Biol.* **2018**, *1*, 199.
[17] H. Vandenburgh, J. Shansky, F. Benesch-Lee, V. Barbata, J. Reid, L. Thorrez, R. Valentini, G. Crawford, *Muscle Nerve* **2008**, *37*, 438.
[18] A. Bettadapur, G. C. Suh, N. A. Geisse, E. R. Wang, C. Hua, H. A. Huber, A. A. Viscio, J. Y. Kim, J. B. Strickland, M. L. McCain, *Sci. Rep.* **2016**, *6*, 28855.
[19] H. Takahashi, T. Shimizu, T. Okano, *Sci. Rep.* **2018**, *8*, 13932.
[20] K. Ronaldson-Bouchard, K. Yeager, D. Teles, T. Chen, S. Ma, L. J. Song, K. Morikawa, H. M. Wobma, A. Vasciaveo, E. C. Ruiz, M. Yazawa, G. Vunjak-Novakovic, *Nat. Protoc.* **2019**, *14*, 2781.

[21] R. K. Christensen, C. Von Halling Laier, A. Kiziltay, S. Wilson, N. B. Larsen, *Biomacromolecules* **2020**, *21*, 356.
[22] M. E. Afshar, H. Y. Abraha, M. A. Bakooshli, S. Davoudi, N. Thavandiran, K. Tung, H. Ahn, H. J. Ginsberg, P. W. Zandstra, P. M. Gilbert, *Sci. Rep.* **2020**, *10*, 6918.
[23] R. P. Rimington, A. J. Capel, K. F. Chaplin, J. W. Fleming, H. C. H. Bandulasena, R. J. Bibb, S. D. R. Christie, M. P. Lewis, *ACS Biomater. Sci. Eng.* **2019**, *5*, 5525.
[24] A. J. Capel, R. P. Rimington, J. W. Fleming, D. J. Player, L. A. Baker, M. C. Turner, J. M. Jones, N. R. W. Martin, R. A. Ferguson, V. C. Mudera, M. P. Lewis, *Front. Bioeng. Biotechnol.* **2019**, *7*, 20.
[25] E. van der Wal, A. J. Bergsma, T. J. M. van Gestel, S. L. M. in 't Groen, H. Zaehres, M. J. Araúzo-Bravo, H. R. Schöler, A. T. van der Ploeg, W. W. M. P. Pijnappel, *Mol. Ther.-Nucleic Acids* **2017**, *7*, 101.
[26] E. van der Wal, P. Herrero-Hernandez, R. Wan, M. Broeders, S. L. M. In 't Groen, T. J. M. van Gestel, W. F. J. van IJcken, T. H. Cheung, A. T. van der Ploeg, G. J. Schaaf, W. W. M. P. Pijnappel, *Stem Cell Rep.* **2018**, *10*, 1975.
[27] U. N. Lee, X. Su, D. J. Guckenberger, A. M. Dostie, T. Zhang, E. Berthier, A. B. Theberge, *Lab Chip* **2018**, *18*, 496.
[28] X. Ma, R. Li, Z. Jin, Y. Fan, X. Zhou, Y. Zhang, *Microsyst. Technol.* **2020**, *26*, 1317.
[29] V. Saggiomo, A. H. Velders, *Adv. Sci.* **2015**, *2*, 1500125.
[30] R. F. Shepherd, F. Ilievski, W. Choi, S. A. Morin, A. A. Stokes, A. D. Mazzeo, X. Chen, M. Wang, G. M. Whitesides, *Proc. Natl. Acad. Sci. USA* **2011**, *108*, 20400.
[31] F. Ilievski, A. D. Mazzeo, R. F. Shepherd, X. Chen, G. M. Whitesides, *Angew. Chem., Int. Ed.* **2011**, *50*, 1890.
[32] S. B. J. Willems, J. Zegers, A. Bunschoten, R. M. Wagterveld, F. W. B. van Leeuwen, A. H. Velders, V. Saggiomo, *Analyst* **2020**, *145*, 1629.
[33] K. Shimizu, R. Genma, Y. Gotou, S. Nagasaka, H. Honda, *Bioengineering* **2017**, *4*, 56.